Synthesis mechanism of heterovalent Sn_2O_3 nanosheets in oxidation annealing process*

Zhao Jun-Hua(赵俊华)[a)†], Tan Rui-Qin(谭瑞琴)[b)], Yang Ye(杨 晔)[c)], Xu Wei(许 炜)[c)], Li Jia(李 佳)[c)], Shen Wen-Feng(沈文峰)[c)], Wu Guo-Qiang(吾国强)[a)], Yang Xu-Feng(杨旭峰)[a)], and Song Wei-Jie(宋伟杰)[c)]

[a)] *College of Chemical and Material Engineering, Quzhou University, Quzhou* 324000, *China*
[b)] *Faculty of Information Science and Engineering, Ningbo University, Ningbo* 315211, *China*
[c)] *Ningbo Institute of Material Technology and Engineering, Chinese Academy of Sciences, Ningbo* 315201, *China*

(Received 27 November 2014; revised manuscript received 5 May 2015; published online 18 May 2015)

Heterovalent Sn_2O_3 nanosheets were fabricated via an oxidation annealing process and the formation mechanism was investigated. The temperature required to complete the phase transformation from Sn_3O_4 to Sn_2O_3 was considered. Two contrasting experiments showed that both oxygen and heating were not necessary conditions for the phase transition. Sn_2O_3 was formed under an argon protective atmosphere by annealing and could also be obtained at room temperature by exposing Sn_3O_4 in atmosphere or dispersing in ethanol. The synthesis mechanism was proposed and discussed. This fundamental research is important for the technological applications of intermediate tin oxide materials.

Keywords: intermediate tin oxides, nanosheets, metastable phase, synthesis mechanism

PACS: 05.70.Fh, 64.60.My, 62.23.Kn **DOI:** 10.1088/1674-1056/24/7/070505

1. Introduction

Smart and functional oxide materials with heterovalent cation states have attracted a great deal of attention due to their amazing electrical, optical, magnetic, and chemical properties.[1–3] These materials can be used to fabricate smart devices for important technological applications. As a key functional metal oxide, intermediate tin oxides SnO_{2-x} $(0 < x < 1)$ have received increasing attention for their potential applications in gas sensing, catalysts, luminescence, and lithium ion batteries.[4–6] It is noteworthy that the only known preparation method for intermediate tin oxides is the traditional solid-state reactions: decomposition of SnO or carbothermal reduction of SnO_2.[7–9] However, the intermediate oxide phase is always accompanied by other phases, such as stoichiometric tin oxides Sn_3O_4 and metallic tin.[10,11] Sn_2O_3 has been only mentioned as an impurity phase in a liquid-phase method.[12–14] Pure phase Sn_2O_3 has not been obtained yet.

Solution-phase chemical routes can be used to provide materials with high purity and nanoscale crystalline.[15] The hydrothermal synthesis has been proved to be an effective method for preparing mixed-valence compounds of transition metals.[16] Sn_3O_4 nanosheets were first synthesized by our laboratory under hydrothermal conditions using stannous chloride as the source.[17–19] Sn_2O_3-based sensors were fabricated by Sn_3O_4 dispersion later, showing high selectivity for NO detection.[17] To our knowledge, there are very few reports about the synthesis mechanism of the mixed-valence crystalline phase of Sn_2O_3 due to the lack of pure phase.[12–14]

In this study, the formation process of Sn_2O_3 is studied in detail and two contrasting experiments are carried out. Through the analysis of the experimental study, the synthesis mechanism of Sn_2O_3 nanosheets is discussed.

2. Experiment

To prepare the Sn_3O_4 nanosheets, 0.12 mol $SnCl_2{\cdot}2H_2O$ (AR, SCRC, China) was dissolved into 200 mL distilled water and the pH value was regulated to 11.80 by 0.50 mol/L NaOH under vigorous magnetic stirring for 2 h.[17] The obtained mixture was transferred into a 100 mL Teflon-lined stainless autoclave, sealed and maintained at 180 °C for 12 h, then cooled down to room temperature. The obtained precipitates were centrifuged and washed six times with water and ethanol until Cl ions could not be detected. The products were finally dried in a vacuum at 60 °C for 1 h. Sn_3O_4 nanosheets were further annealed at 300 °C for 1 h at oxygen atmosphere until totally transferred to Sn_2O_3. To show the oxidation process of Sn_3O_4 nanosheets, the powders were annealed at 137 °C, 435 °C, 550 °C, and 740 °C respectively for 1 h in oxygen atmosphere. Sn_3O_4 nanosheets annealed under argon protective atmosphere were also synthesized. The powders were sealed in a silicon vacuum tube, annealed at 300 °C and 500 °C for 1 h at the vacuum levels of 1.0×10^5 Pa, 5.7 Pa, and 4.1×10^{-4} Pa, respectively, and slowly cooled down to room temperature. The Sn_3O_4 dispersion was synthesized by magnetically stirring for 1 h, followed by ultrasonic agitation at 40 kHz (300 W) for 30 min at room temperature.

*Project supported by the National Natural Science Foundation of China (Grant Nos. 21377063, 51102250, 21203226, and 21205127) and the Personnel Training Foundation of Quzhou University, China (Grant No. BSYJ201412).

†Corresponding author. E-mail: Zhaojh1018@163.com

© 2015 Chinese Physical Society and IOP Publishing Ltd

The phase identification was achieved by x-ray diffraction (XRD) using a Bruker AXS D8 advance diffractometer with Cu $K\alpha$ radiation at a power of 1.6 kW. High-resolution transmission electron microscopy (HRTEM) and selected area electron diffraction (SAED) patterns were obtained with an FEI Tecnai F20 field emission electron microscope. XPS spectra were obtained using a Kratos Axis Ultra DLD XPS system. Thermogravimetric analyses (TG, Pyris Diamond TG/DTA, Perkin-Elmer, USA) were conducted for the samples with a heating rate of 2 °C/min. The Fourier transform infrared (FTIR) spectra of the nanoparticles were collected using a Thermo Electron Nicolet 6700 spectrometer (Nicolet 6700, Thermo Electron Corporation, Madison, WI). The optical transmission spectra were recorded using an ultraviolet–visible–near–infrared (UV–visible–NIR) spectrometer (Perkin Elmer Lambda 950, Shelton, USA) in the wavelength range of 190–400 nm.

3. Results and discussion

3.1. Structural and morphology analysis

Figure 1 shows the typical XRD patterns of the as-synthesized products obtained by annealing Sn_3O_4 nanosheets at 300 °C for 1 h. The XRD patterns cannot be indexed to either tin oxide or stannous oxide, while they are similar to anorthic-phase Sn_3O_4 (JCPDS No. 16-0737) and Sn_2O_3 (JCPDS No. 25-1259). Comparing to the standard XRD spectrum of Sn_3O_4, peaks of (102) and (013) disappear, peaks of (010), (111), $(\bar{1}32)$, and $(0\bar{3}3)$ stay the same, while the other peaks all shift significantly to higher angles (ca. 0.34°). The spectrum is also similar to that of Sn_2O_3 (JCPDS No. 25-1259). The diffraction peaks of the JCPDS card at angles higher than 58° disappear because of the conversion of radiation from Cr $K\alpha$ ($\lambda = 2.2897$ Å) to Cu $K\alpha$ ($\lambda = 1.5418$ Å). Figure 2 shows HRTEM and SEM images of the as-synthesized products. The nanoparticle shows a sheet-like morphology and exhibits a single-like diffraction pattern, implying that it is highly crystalline with a lattice spacing of 2.46 nm.

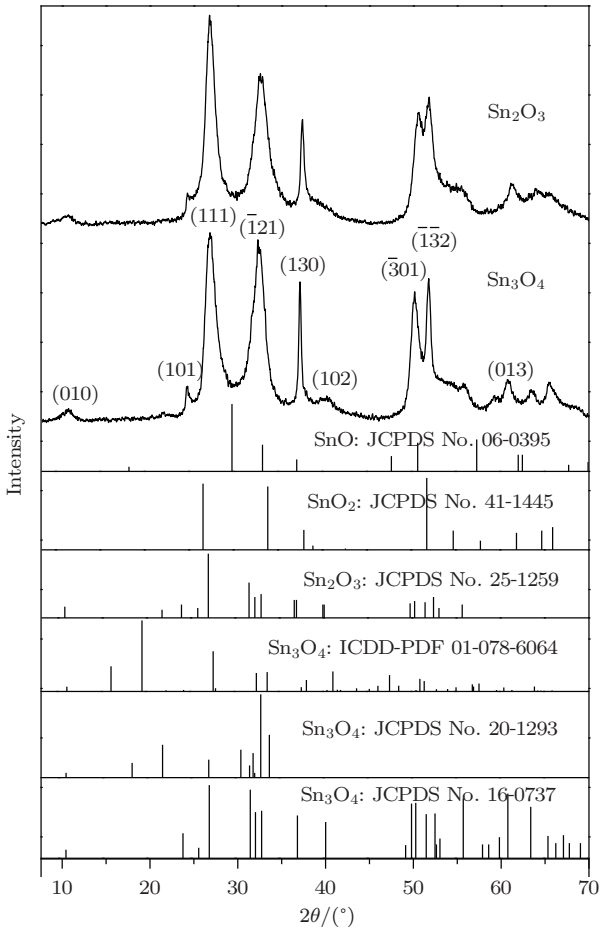


Fig. 1. XRD patterns of Sn_3O_4 nanosheets annealed under oxygen atmosphere at 300 °C for 1 h.

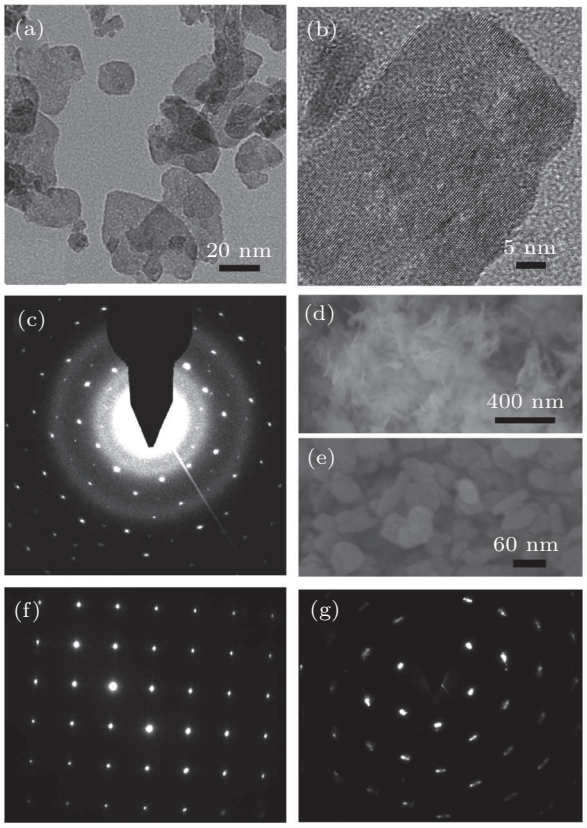


Fig. 2. (a) TEM, (b) HRTEM, and (c) SAED images of Sn_3O_4 nanosheets annealed under oxygen atmosphere at 300 °C for 1 h. (d) and (e) SEM images of Sn_3O_4 nanosheets before and after annealing. (f) and (g) Typical SAED patterns of SnO and SnO_2 particles.

Figure 3(a) shows the curve-fitting data of the Sn 3d core-level spectra. The area ratio of $S = S(Sn^{2+})/[S(Sn^{4+}) + S(Sn^{2+})]$ is 0.49 deduced from the Sn 3d spectra. It means that this nanosheet contains similar concentrations of Sn^{2+} and Sn^{4+}.[20] In addition, Sn 3d and O 1s spectra show that the ratio of O/Sn is 1.48. These results are also confirmed by the valence-band (VB) spectrum (Fig. 3(b)). Owing to the prominent Sn 5s-derived peak characteristic of Sn^{2+} from the VB spectrum, $I = I(\text{Sn 5s})/I(\text{O 2p})$ has been used to monitor the

approximate concentrate ratio of Sn^{2+}.[21] Using the value of $I_{Sn_3O_4}/I_{SnO_{2-x}} = 1.43$ derived from the VB specturm, we expect ratio S to be 0.47 for SnO_{2-x}. Generally, the above results indicate that the as-prepared nanosheet is Sn_2O_3.[17]

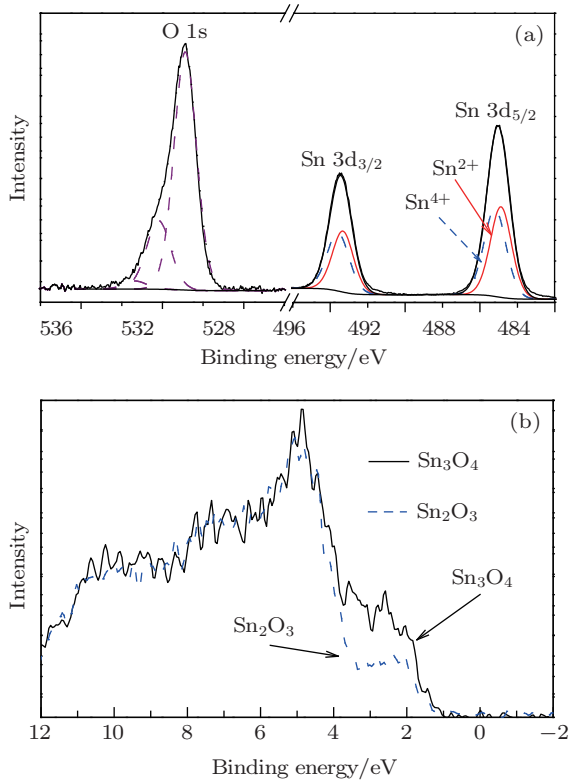


Fig. 3. (color online) (a) XPS spectra and (b) valence-band spectrum of Sn_3O_4 nanosheets annealed under oxygen atmosphere at 300 °C for 1 h.

3.2. Oxidation properties

Thermogravimetric-differential thermal analysis (TG-DTA, Fig. 4.) is used to evaluate the oxidation properties of Sn_3O_4. Under air flow and a 2 °C/min ramp rate, TG-DTA reveals a rapid weight loss at 185 °C, which is due to the loss of moisture. The reason for the change of weight at the temperature higher than 400 °C is the adsorption and desorption of adsorbed oxygen at the surface of the particle.[22] This result agrees well with the linear relationship between the adsorbed oxygen content obtained from XPS and the sample weight. With the increase of temperature, Sn_3O_4 is oxidized with the decrease of the Sn^{2+}/Sn^{4+} ratio, and finally a phase transition to rutile-type SnO_2 occurs at 550 °C during thermal processing. Furthermore, the weight is stable from 286 °C to 381 °C, where Sn_2O_3 is detected. This result agrees perfectly with the prediction by first principles that Sn_2O_3 is the second metastable phase with formation energy of −8 meV/Sn.[23]

To further understand the formation mechanism of Sn_2O_3, a contrasting experiment was carried out. The Sn_3O_4 nanosheets were annealed under the argon protective atmosphere with the vacuum levels of 10^5 Pa to 10^{-4} Pa at 300 °C. With the increase of the vacuum level, the oxidation process of Sn_3O_4 is delayed (Fig. 5). By increasing the temperature from 300 °C to 500 °C, Sn_2O_3 is synthesized with the vacuum levels of 10^1 Pa to 10^{-4} Pa. These results indicate that oxygen is not the necessary condition for the preparation of Sn_2O_3.

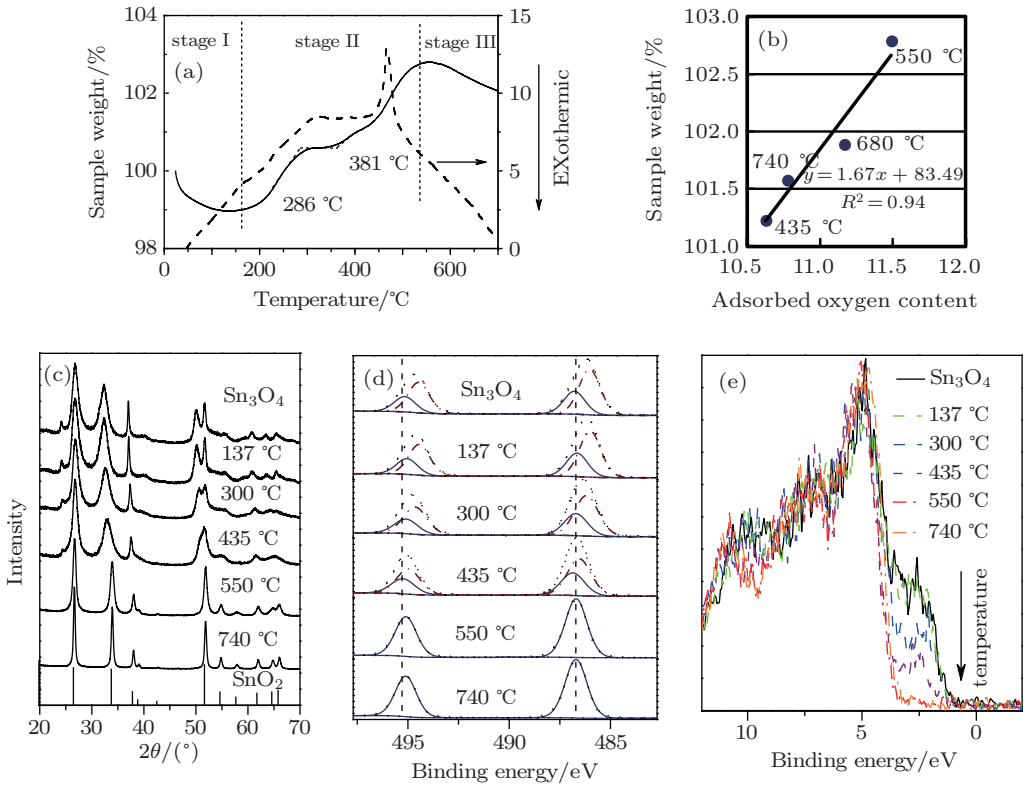


Fig. 4. (color online) (a) TG curve, (b) adsorbed oxygen content from XPS verus sample weight, (c) XRD, (d) XPS patterns, and (d) valence-band XPS spectra of Sn_3O_4 annealed at various temperatures at a 5 °C/min ramp rate.

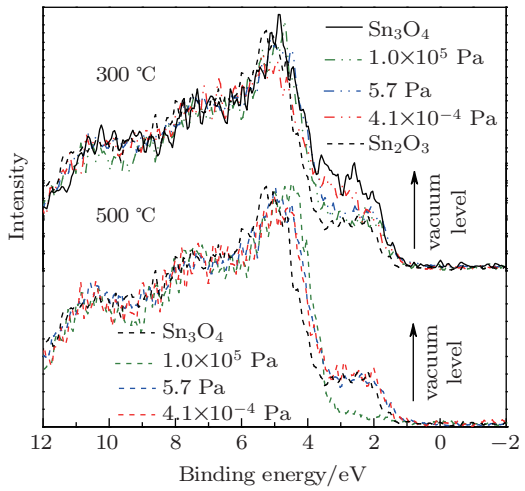


Fig. 5. (color online) The valence-band XPS spectra of Sn_3O_4 annealed under argon protective atmosphere at 300 °C and 500 °C with the vacuum levels of 10^5 Pa to 10^{-4} Pa.

3.3. Formation mechanism of Sn_2O_3 nanosheets

To determine which parameters affect the oxidation process from Sn_3O_4 to Sn_2O_3, we investigated the oxygen-free heating progress. By exposing Sn_3O_4 nanosheets in dry air at room temperature, the light greenish-yellow Sn_3O_4 nanosheets turned brown and converted to Sn_2O_3 after 12 months (Fig. 6). By comparing to the data in Fig. 3, it is found that the annealing process depends on the oxidation kinetics.

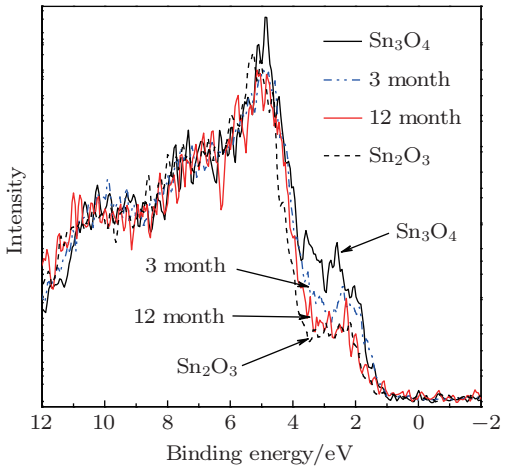


Fig. 6. (color online) The valence-band XPS spectra of Sn_3O_4 after exposing in the atmosphere for one year.

Similarly, the fresh Sn_3O_4-ethanol dispersion turned brown by standing at room temperature. The ratio of Sn^{2+}/Sn^{4+} decreased during standing time and Sn_2O_3 was synthesized within 7 days (Fig. 7). Figure 8(a) shows the FTIR spectra of the Sn_3O_4–ethanol dispersion with different exposing time. For all samples, three strong bands exist around 650 cm^{-1}, which are ascribed to Sn–O vibration.[24] The broad absorption peaks centered at 3425 cm^{-1} and 1629 cm^{-1} are attributed to −OH stretching and bending modes,[25] respectively. The bands of $-CH_2$ and $-CH_3$ stretching modes do not appear in the FTIR spectra, which indicates that ethanol is not chemisorbed on the Sn_3O_4 nanosheets. Furthermore, an absorption peak appears at 1102 cm^{-1} and becomes stronger during the exposing time, which is assigned to the superoxide radical anion (O_2-) stretching modes.[26]

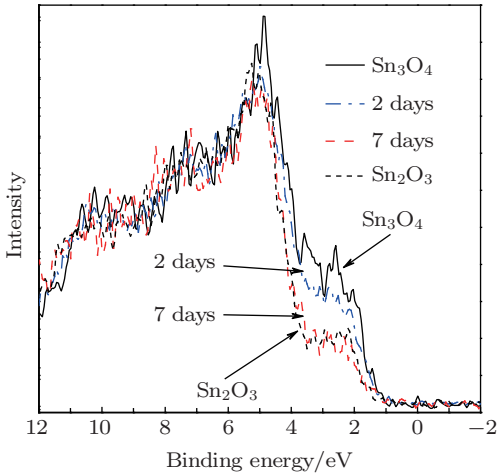


Fig. 7. (color online) The valence-band XPS spectra of Sn_3O_4 after exposing in ethanol for 7 days.

Figure 8(b) shows the UV–vis spectra of Sn_3O_4–ethanol dispersion with different exposing time. An extra absorption band near 204 nm appears after 2 days. This peak might correspond to Sn^{4+} species,[27] and increases with the increase of exposing time in Fig. 8(b). This means that Sn^{2+} is oxidized to Sn^{4+} with the increase of exposing time, which agrees well with the valence-band XPS spectra.

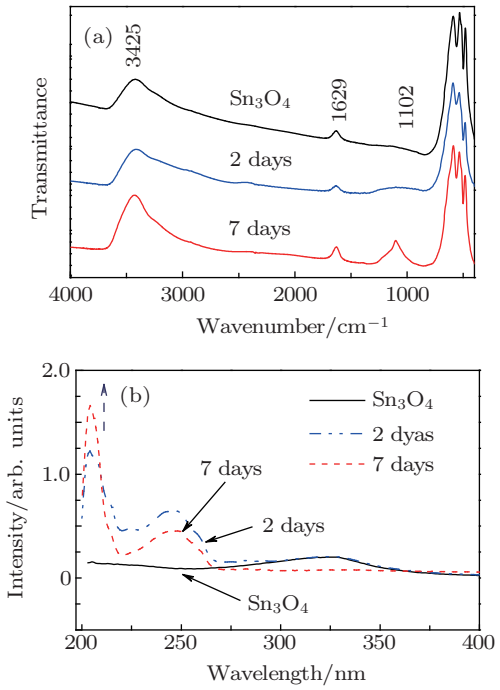


Fig. 8. (color online) (a) The Fourier transform infrared spectra and (b) UV–vis absorption spectra of Sn_3O_4 after exposing in ethanol for seven days.

The formation mechanism of Sn_2O_3 synthesized by annealing Sn_3O_4 under air at 300 °C could be explained as

follows. The oxygen vacancies layered on the (101) planes may be suitable sites available for oxygen adsorption. The chemisorption of oxygen may result in a mixture of various oxygen species on the surface, expressed as $O_{2(g)}$ + V_O + e^- ⇔ adsorbed oxygen, where e^- is the quasi-free electron. The annealing process induces the surface oxygen vacancies, which trap the electrons from adsorbed oxygen and react with gaseous oxygen according to the following reaction: $\frac{1}{2}O_{2(g)}$ + O^{2-} + $V_O \rightarrow 2O_O^x$, where O_O^x is the atomic oxygen. The oxygen vacancy disappears with the decrease of the bond length between Sn and O ions. A more stable structure exists with higher bond energies.

When dispersing Sn_3O_4 into ethanol, the surface oxygen vacancies trap the electrons from ethanol, which breaks down the balance of long pairs between Sn and O ions.[28] This may be the reason why the peak near 204 nm in Fig. 8(b) appears after 2 days' exposure in ethanol. The metastable structure distorts and tends to a more stable structure with the formation of oxygen vacancy. The detailed interaction behavior between Sn_3O_4 and ethanol needs further exploration.

4. Conclusion

The heterovalent Sn_2O_3 nanosheet was synthesized by oxidation of Sn_3O_4 at 300 °C for 1 h at oxygen atmosphere. This was supported by XRD, HRTEM, and XPS studies, which showed that the synthesized nanosheet has high crystalline and contains similar concentrations of Sn^{2+} and Sn^{4+} species. Neither the oxygen nor the heating processes were necessary for the fabrication of Sn_2O_3. Sn_2O_3 could be obtained by annealing Sn_3O_4 under an argon protective atmosphere with different vacuum levels, and also could be synthesized at room temperature by exposing Sn_3O_4 in the atmosphere or dispersing in ethanol. The synthesis mechanism was proposed and characterized. These experimental results extended the knowledge base that can be used to guide technological applications of intermediate tin oxide materials.

References

[1] Hu Y, Li J C, Shen M W and Shi X Y 2014 *Chin. Phys. B* **23** 78704
[2] He J H, Wu T H, Hsin C L, Li K M, Chen L J, Chueh Y L, Chou L J and Wang Z L 2006 *Small* **2** 116
[3] Li X Q, Zheng L and Wang X F 2014 *Chin. Phys. Lett.* **31** 024701
[4] Stankiewiez J, Villuendas F and Bartolomé J 2007 *Phys. Rev. B* **75** 235308
[5] Wang G X, Takeguchi T, Yamanaka T, Muhamad E N, Mastuda M and Ueda W 2010 *Appl. Catal. B: Environ.* **98** 86
[6] Heo J, Hock A S and Gordon R G 2010 *Chem. Mater.* **22** 4964
[7] Lawson F 1967 *Nature* **215** 955
[8] White T A, Moreno M S and Midgley P A 2010 *Z. Kristallogr.* **225** 56
[9] Berengue O M, Simon R A, Chiquito A J, Dalmaschio C J, Leite E R, uerreiro G H A and Guimaraes F E G 2010 *J. Appl. Phys.* **107** 033717
[10] Murken G and Tromel M 1973 *Z. Anorg. Allg. Chem.* **397** 117
[11] Hasselbach K, Murken G and Tromel M 1973 *Z. Anorg. Allg. Chem.* **397** 127
[12] Choi W K, Sung H, Kim K H, Cho J S, Choi S C, Jung H J, Koh S K, Lee C M and Jeong K 1997 *J. Mater. Sci. Lett.* **16** 1551
[13] Beisenkhanov 2011 *Phys. Solid State* **53** 390
[14] Chen T S, Huang K L and Pan Y C 2012 *Int. J. Electrochem. Sci.* **7** 11191
[15] O'Brien S, Brus L and Murray C B 2001 *J. Am. Chem. Soc.* **123** 12085
[16] Cao M H, Hu C W, Peng G, Qi Y J and Wang E B 2003 *J. Am. Chem. Soc.* **125** 4982
[17] Zhao J H, Tan R Q, Shen W F, Yang Y, Guo Y Q, Li J, Zhou Z, Jian J W and Song W J 2012 *Mater. Lett.* **84** 94
[18] Xu W, Li M, Chen X B, Zhao J H, Tan R Q, Li R, Li J and Song W J 2014 *Mater. Lett.* **120** 140
[19] Li M, Tan R Q, Li Rong, Song W J and Xu W 2014 *Ceram. Int.* **40** 11381
[20] Zenkyu R, Tajima D and Yuhara J 2012 *J. Appl. Phys.* **111** 064907
[21] Themlin J M, Chtaib M, Henrard L, Lambin P, Darville J and Gilles J M 1992 *Phys. Rev. B* **46** 2460
[22] Rusu C N and Yates J T 1997 *Langmuir* **13** 4311
[23] Seko A, Togo A, Oba F and Tanaka I 2008 *Phys. Rev. Lett.* **100** 045702
[24] Wang L, Wang D, Dong Z H, Zhang F X and Jin J 2014 *Small* **10** 998
[25] Zhao J H, Tan R Q, Zhang Y L, Yang Y, Guo Y Q, Zhang X P, Wang W Y and Song W J 2011 *J. Am. Ceram. Soc.* **94** 725
[26] Andrews L and Smardzewski R R 1973 *J. Chem. Phys.* **58** 2258
[27] Popescu D A, Herrmann J M, Ensuque A and Verduraz F B 2001 *Phys. Chem. Chem. Phys.* **3** 2522
[28] Röder H, Zang J and Bishop A R 1996 *Phys. Rev. Lett.* **76** 1356